

Study of the influence of the polyalcohol mannitol on zinc electrodeposition from an alkaline bath

M. F. de Carvalho · W. Rubin · I. A. Carlos

Received: 8 October 2009 / Accepted: 25 April 2010 / Published online: 9 May 2010
© Springer Science+Business Media B.V. 2010

Abstract In this paper, the effects of adding mannitol to an alkaline plating bath on the electrodeposition of zinc onto AISI 1010 steel are described and assessed. From cyclic voltammograms with various lower-limit potentials, it is concluded that an initial zinc bulk deposition (region of wave c_0) occurs from -1.45 V in the negative sweep. When the sweep is reversed at -1.60 V, an anodic peak a_1 is seen in the positive sweep both in the absence and in presence of mannitol, which was assigned to zinc dissolution. This peak indicates that the primary nucleation and growth of zinc in region c_0 is followed by zinc secondary nucleation and growth (region of peak c_1). Scanning electron micrographs show that zinc electrodeposits obtained at mannitol concentrations ≥ 0.10 M were more refined than at lower concentrations. Energy-dispersive X-ray spectroscopy of these electrodeposits show oxygen contents that are generally low or below detection limit.

Keywords Zinc · Electrodeposition · Mannitol · Alkaline media · Steel substrate · Voltammetry

1 Introduction

In view of valuable features such as its ability to protect steel from corrosion, zinc has been widely used as a coating in industry [1]. Also, the Zn anode is very attractive

for battery applications, as it has a high negative potential, is non-toxic, abundant, and relatively stable in alkaline media [2, 3]. However, the value of zinc coatings, for example as a sacrificial coating or as a good base on steel for painting, depends on the absence of dendritic growth, since dendrites weaken the coating.

Zinc has been electrodeposited from various alkaline solutions including zincate without additives [4] or with additives such as the following: $C_6F_{13}C_2H_4(OC_2H_4)_{12}OH$ and $C_{12}H_{25}(C_2H_4O)_{12}H$ [5]; a tetraalkylammonium salt [6, 7]; ammine-oxalate-EDTA [8]; tetramethylammonium, tetrabutylammonium or benzyl alcohol [9]; glycerol [10], and sorbitol [11]. Alkaline electrolytes are preferable not only from the point of view of environmental protection but also for their low corrosiveness, compared to acid electrolytes.

We have been studying the electrodeposition of zinc onto AISI 1010 steel from alkaline solutions containing various polyalcohol additives, since we noted that the presence of sorbitol or glycerol in an alkaline deposition bath has a beneficial effect on the quality of Zn [10, 11], Pb [12], Sn [13], and Cu [14, 15] electrodeposits. In these experiments, it has been established that the presence of sorbitol in the bath leads to the formation of light-gray zinc films, even during the evolution of hydrogen, without cracks or dendrites [11]; reduces the propagation of dendritic growth of lead, refining the lead deposit and allowing the new electrolytic solution to be used to recycle lead scrap [12]; works as a brightener, since tin crystallites were much smaller than those obtained from an alkaline solution without sorbitol [13], and leads to smaller-copper crystallites and a smoother copper film, with a golden color [14, 15]. When glycerol was added to a zinc deposition bath, good values of current efficiency (CE) were observed and zinc deposits were adherent [10].

M. F. de Carvalho · W. Rubin · I. A. Carlos (✉)
Departamento de Química, Universidade Federal de São Carlos,
CP 676, São Carlos, SP 13565-905, Brazil
e-mail: diac@ufscar.br

Another polyalcohol additive investigated in our laboratory is mannitol [16], in the electrodeposition of ZnNi alloy. The results were excellent, since the ZnNi deposits were composed of coalesced globular grains, smaller than $\sim 1 \mu\text{m}$ in diameter. The Ni content in the ZnNi deposits produced in the presence of mannitol was raised from 6 to 10 wt% in the potential range -1.26 to -1.40 V. It was suggested that the ZnNi deposits obtained in these baths probably offered sacrificial protection to the substrate (steel). Also, these results corroborated those for ZnNi electrodeposition in the presence and absence of glycerol or sorbitol [17].

Here, we investigated the use of mannitol as an additive in a zinc plating bath. The choice of this additive resides in the fact that mannitol showed excellent results on the electrodeposition of ZnNi alloy [16], while its effects in the electrodeposition of zinc alone have not been investigated. In this context and continuing our former studies, in this paper, we review the production of zinc electrodeposits on a 1010 steel substrate in an alkaline bath containing mannitol, with particular emphasis on the optimization of the new electrolytic solution and deposition conditions to obtain zinc electrodeposits without dendrites.

2 Experimental

All chemicals were of analytical grade. Double-distilled water was used throughout. Each electrochemical experiment was performed in an alkaline bath containing 0.10 M $\text{ZnSO}_4 \cdot 7\text{H}_2\text{O} + 2.0$ M NaOH, with various mannitol concentrations (0.0, 0.0050, 0.010, 0.10, and 0.20 M). An AISI 1010 steel disk (0.407 cm^2), a Pt plate, and a $\text{Hg}/\text{Hg}_2\text{Cl}_2/0.10$ M KCl electrode with an appropriate Luggin capillary were employed as working, auxiliary, and reference electrodes, respectively. The AISI 1010 steel, from CSN Co. (Brazil), contained 0.04% P, 0.08% C, 0.3% Mn, and 0.05% S. Immediately prior to the electrochemical measurements, the working electrode was ground with 600 emery paper and rinsed with distilled water. The CE was calculated from the stripping/deposition charge ratio. In these tests, the Zn was deposited up to charge densities of 2.0 and 10.0 C cm^{-2} and then stripped in a solution of 1.0 M NH_4NO_3 . Potentiodynamic curves were recorded with a GAMRY PCI-4 750 mA potentiostat/galvanostat. All experiments were carried out at room temperature (25 °C). Scanning electron microscopy (SEM) photographs were taken with a Phillips (model XL 30 Oxford TMP) electron microscope. Energy-dispersive X-ray spectroscopy (EDS) measurements were made with a Zeiss/Leica LEO 440 microscope and an EDS Si/Li device with an ultrathin Be window.

3 Results and discussion

3.1 Electrodeposition of Zn on steel substrate

Figure 1 shows voltammograms recorded from the 1010 steel substrate in electrolytic solutions containing 0.10 M ZnSO_4 , 2.0 M NaOH, and various mannitol concentrations. In the deposition arm of these voltammograms, a cathodic wave extends from -0.70 V to about -1.52 V (c_0) and a cathodic peak can be seen at around -1.56 V (c_1). The wave c_0 is associated with the hydrogen evolution reaction (HER) on steel and reduction of iron oxide (as can be seen better in Fig. 2), as well as initial zinc bulk deposition on the steel. The peak c_1 refers to secondary zinc bulk deposition. In the positive sweep, an anodic peak, a_1 , of zinc dissolution can be seen, both in the presence and absence of mannitol.

Figure 1 and Table 1 show that at peak c_1 , the current density (j) did not vary significantly with mannitol concentration. In the region of wave c_0 , however, j increased with increasing mannitol concentration; for example, at -1.50 V, the values of j were 1.89 mA cm^{-2} (without mannitol) and 3.60 mA cm^{-2} (at 0.20 M mannitol). Thus, the added mannitol affected the processes occurring in the region of wave c_0 . The potential of peak c_1 shifted by 20 mV in the positive direction (from -1.57 V to -1.55 V) as the mannitol concentration rose from 0 to 0.10 M.

The constancy of j_{c_1} seen in Fig. 1 and Table 1 suggests that the surface area of the zinc electrodeposit obtained in the region of peak c_1 , in the absence or presence of mannitol, did not vary significantly. Beyond the potential of

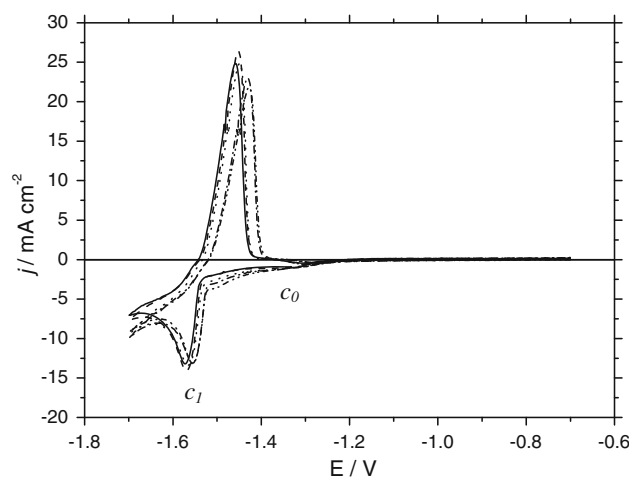


Fig. 1 Voltammetric curves of deposition and dissolution of zinc, on a 1010 steel electrode, obtained in solutions of 0.10 M $\text{ZnSO}_4 + 2.0$ M NaOH, containing various concentrations of mannitol: (—) 0.0 M; (—) 0.0050 M; (···) 0.010 M; (-·-) 0.10 M and (-··-) 0.20 M; sweep rate 10.0 mV s^{-1}

Fig. 2 Voltammetric curves obtained in a solution of 2.0 M NaOH, in the absence (—) or presence (---) of 0.20 M mannitol, on a 1010 steel electrode, at 10.0 mV s⁻¹. **a** Negative and positive, **b** negative, and **c** positive sweeps

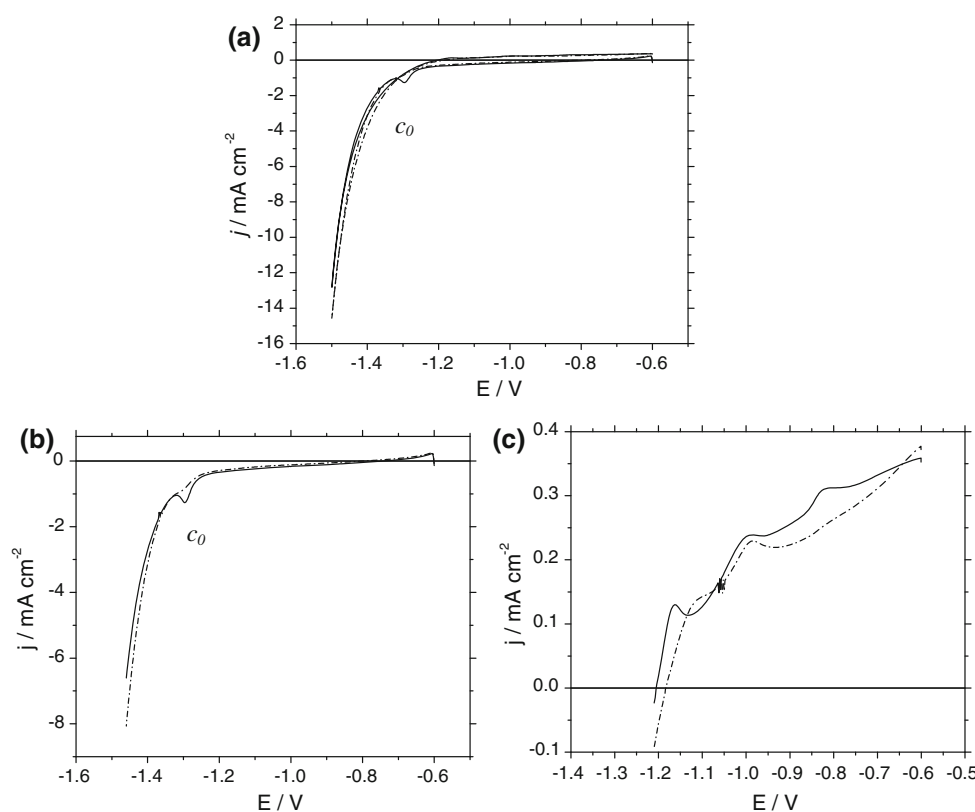


Table 1 Values of the cathodic peak potential and current density for solutions containing 0.10 M ZnSO₄, 2.0 M NaOH and various mannitol concentrations

Mannitol (M)					
	0.0	0.0050	0.010	0.10	0.20
E_{c_1} ^a (V)	-1.57	-1.57	-1.56	-1.55	-1.55
j_{c_1} ^a (mA cm ⁻²)	-13.21	-14.12	-13.37	-13.11	-13.19

^a E_{c_1} cathodic peak potential, j_{c_1} peak current density

peak c_1 (potential region ~ -1.57 V to ~ -1.67 V), j fell, indicating that the deposition in this region was controlled by diffusion. Immediately beyond this region, j increased again, due to the HER on zinc occurring in parallel with the reduction of the zincate anion.

To understand the process occurring in the region of wave c_0 more clearly, cyclic voltammograms, with the lower-limit potential at -1.50 V, were performed on the 1010 steel electrode in a blank solution containing 2.0 M NaOH, without and with 0.20 M mannitol (Fig. 2a). Starting from -0.60 V, under both conditions, there is an increase in j related to the HER ($2\text{H}_2\text{O} + 2\text{e}^- \rightarrow \text{H}_2(\text{g}) + 2\text{OH}^-$) (wave c_0). Also, it can be seen that a cathodic peak (~ -1.30 V) or wave is formed, in the absence and presence of mannitol, respectively (as can be seen better in Fig. 2b).

Tulio and Carlos [18] report that the steel electrode can form an iron oxide film before or during immersion of the

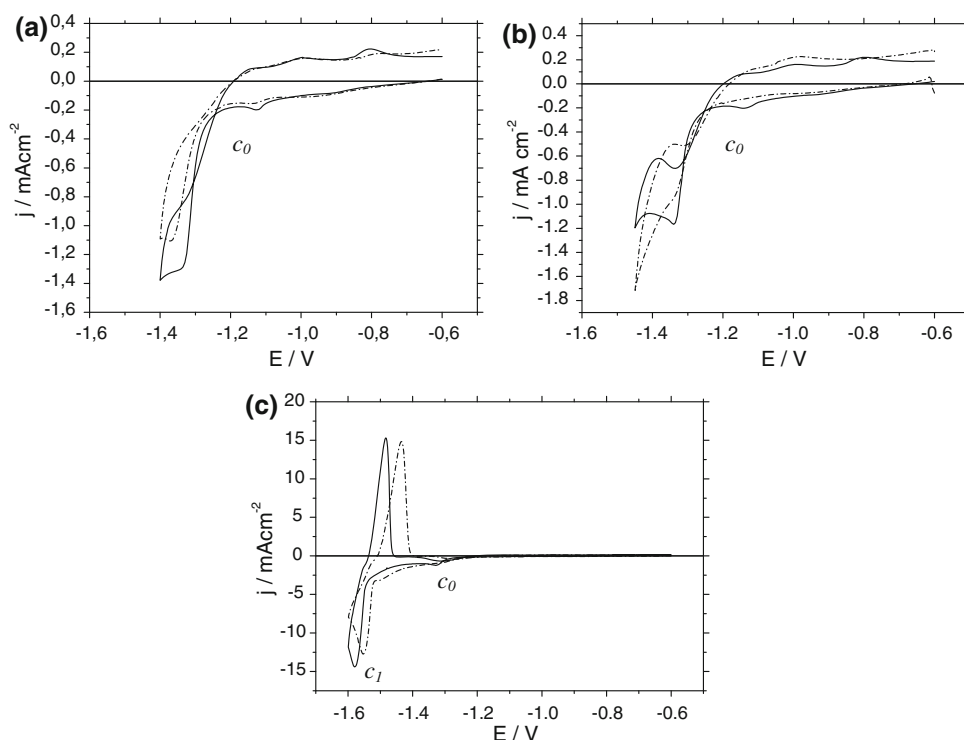
electrode in the electrolytic solution, in both cases without electrode polarization. Thus, the curves in Fig. 2a, b show the reduction of iron oxide film in the negative sweep, in parallel to the HER (seen by naked eye), either in the absence or presence of mannitol, contributing to wave c_0 .

The positive sweep in Fig. 2a shows the occurrence of passivation by oxide formation, in the absence or presence of mannitol, which can be seen better in Fig. 2c. It can also be seen that the mannitol hindered the formation of iron oxide, since the initial dissolution potential was changed to a more positive value. These results can explain why the cathodic peak (~ -1.30 V) becomes a wave (as can be seen better in Fig. 2b) in the presence of mannitol, as the presence of this additive probably depressed the rate of HER and the formation of iron oxide. Similar results were obtained at other mannitol concentrations.

It is reported in the literature that EDTA is known to remove iron oxides. The results obtained here indicate that mannitol may behave similar to EDTA [19, 20].

Cyclic voltammograms of 1010 steel, with limit potentials at -1.40 , -1.45 , and -1.6 V, were produced in solutions containing 0.10 M ZnSO₄ and 2.0 M NaOH, in the absence and presence of 0.20 M mannitol (Fig. 3a, b, c). When the sweep was reversed at -1.40 V (Fig. 3a), no zinc dissolution peak was visible in the positive sweep, indicating that zinc deposition did not occur at this potential. Thus, the region of the cathodic wave between

Fig. 3 Voltammetric curves obtained in the solution 0.10 M $\text{ZnSO}_4 + 2.0\text{ M}$ NaOH , in the absence (—) or presence (---) of 0.20 M mannitol, on a 1010 steel electrode; potential reversed at **a** -1.40 V , **b** -1.45 V , and **c** -1.60 V ; sweep rate 10.0 mV s^{-1}



-0.60 and -1.40 V can be attributed entirely to the HER and reduction of iron oxide. At limit potential -1.45 V (Fig. 3b), it can be seen that, at the start of the return sweep, the current decreases and, at the potential of approximately -1.38 V , increases briefly, then decreases again, with a crossover [21] at $\sim -1.32\text{ V}$, indicating that an initial zinc bulk deposition occurred at -1.45 V , i.e., primary nucleation and growth of zinc in region c_0 . This process became more significant as the negative sweep was reversed at more negative potentials, for example, at -1.50 V and at -1.55 V , since the amount of deposited metal had increased (data not shown).

Thus, it can be inferred from these results that wave c_0 (Fig. 1) corresponds to iron oxide reduction/HER/initial zinc bulk deposition.

Finally, when the sweep was reversed at -1.60 V (Fig. 3c), a peak a_1 is seen in the positive sweep at -1.48 V and -1.43 V , in the absence and presence of 0.20 M mannitol, respectively, which is due to zinc dissolution. Thus, mannitol appears to hinder zinc dissolution, probably by being adsorbed on the zinc electrodeposit, corroborating earlier results of Carlos and co-workers [11], who reported that zinc dissolution was inhibited in the presence of sorbitol.

It must be stressed that the anodic peak, a_1 , indicates that the primary nucleation and growth of Zn (region c_0) is followed by secondary nucleation and growth of zinc (peak c_1). The latter occurs on top of the initial bulk zinc deposit. These results corroborate those obtained by Tulio and

Carlos [18] and Siqueira and Carlos [22]. Similar results were obtained at other mannitol concentrations.

Figure 4 shows voltammetric curves of the 1010 steel substrate in the zinicate bath and in the blank solution (2.0 M NaOH) without (Fig. 4a) or with (Fig. 4b) 0.20 M mannitol, reversed at -1.50 V . It can be seen that the evolution of hydrogen by H_2O reduction is hindered when Zn^{2+} ions are present in the solution, without or with mannitol (region wave c_0). This reflects coverage of the steel surface with the initial bulk-Zn deposit.

Figure 5 and Table 2 show that for a deposition charge density (q_d) of 2.0 C cm^{-2} , the CE of the deposition process remained constant in the range of mannitol concentrations from 0 to 0.010 M , but decreased when the mannitol concentration reached 0.10 M . However, for a q_d of 10.0 C cm^{-2} , CE increased as the mannitol concentration rose from 0 to 0.010 M and subsequently decreased at mannitol concentration $\geq 0.10\text{ M}$. The decrease in CE in both cases at mannitol concentrations $\geq 0.10\text{ M}$ is probably due to increasing competition between mannitol and Zn^{2+} ions for active sites on the 1010 steel. For all deposits, it can be seen that the CE was lower than 54%, owing to the HER in parallel with zinc deposition.

The thickness (δ) of the various zinc electrodeposits (Table 3) corroborates the CE values. In the literature, it is reported that zinc deposits can be obtained from a cyanide bath with δ in the range $2.5\text{--}7.5\text{ }\mu\text{m}$ [23]. This bath operates at high current densities and contains considerable amounts of various additives (NaCN , Na_2CO_3 , NaOH ,

Fig. 4 Voltammograms obtained from the solution
a (—) 2.0 M NaOH and (---) 0.10 M ZnSO₄ + 2.0 M NaOH,
b (—) 2.0 M NaOH + 0.20 M mannitol, (---) 0.10 M ZnSO₄ + 2.0 M NaOH + 0.20 M mannitol, on a 1010 steel electrode; sweep rate 10.0 mV s⁻¹

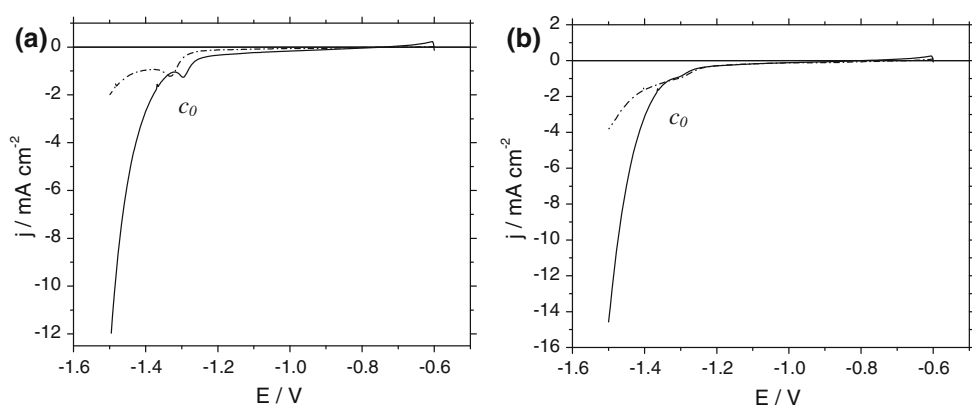


Fig. 5 Current efficiency (CE) for zinc electrodeposits produced chronoamperometrically from −0.60 V to −1.60 V, in the absence or presence of mannitol, for q_d of (▨) 2.0 C cm⁻² and (▨▨) 10.0 C cm⁻²

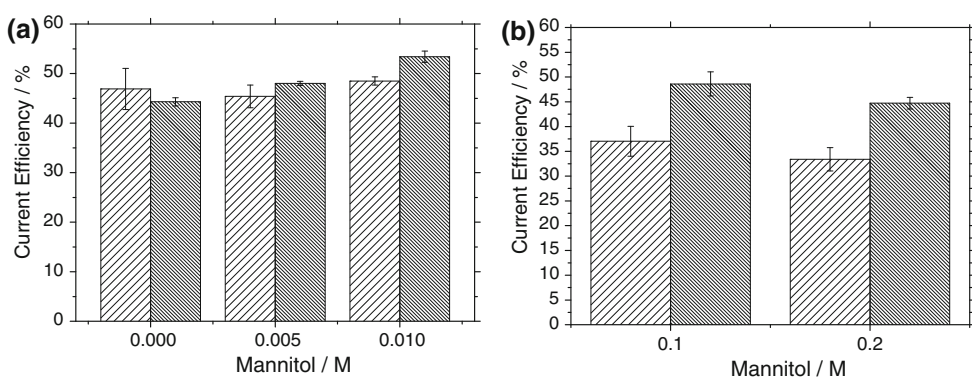


Table 2 Current efficiency (CE) for zinc electrodeposits at two different q_d produced chronoamperometrically from −0.60 V to −1.60 V, at various mannitol contents

Mannitol (M)	CE (%), q_d 2.0 C cm ⁻²	CE (%), q_d 10.0 C cm ⁻²
0.0	46.9 ± 4.2	44.3 ± 0.8
0.0050	45.4 ± 2.3	48.0 ± 0.4
0.010	48.5 ± 0.8	53.4 ± 1.1
0.10	37.0 ± 3.0	48.6 ± 2.4
0.20	33.4 ± 2.4	44.7 ± 1.2

etc.), in contrast to the alkaline zinc bath containing mannitol described here. The thicknesses of the zinc deposits reported here were comparable to those obtained from the cyanide bath, but the mannitol alkaline bath has the advantage of low toxicity, fewer additives, and low-deposition current density.

The CE values for q_d 2.0 and 10.0 C cm⁻² imply that the HER contribution to the cathodic current was similar for both q_d , at mannitol concentrations from 0 to 0.010 M. However, at ≥ 0.10 M mannitol, the contribution of HER was lower for q_d 10.0 C cm⁻², since (as can be seen in Table 3) these deposits were 7 times thicker than those obtained with q_d 2.0 C cm⁻², indicating that the zinc coverage may be greater than other conditions. Thus, at a high mannitol content, when q_d = 10.0 C cm⁻², probably

Table 3 Thickness of zinc electrodeposits at two different q_d produced chronoamperometrically from −0.60 V to −1.60 V, at various mannitol contents

Mannitol (M)	δ (μm), q_d 2.0 C cm ⁻²	δ (μm), q_d 10.0 C cm ⁻²
0.0	0.45 ± 0.04	2.10 ± 0.04
0.0050	0.43 ± 0.02	2.28 ± 0.02
0.010	0.46 ± 0.01	2.54 ± 0.05
0.10	0.36 ± 0.02	2.31 ± 0.12
0.20	0.32 ± 0.02	2.13 ± 0.06

a smaller area of the 1010 steel surface was free for the HER to take place than when q_d = 2.0 C cm⁻².

3.2 Morphological study of zinc electrodeposits

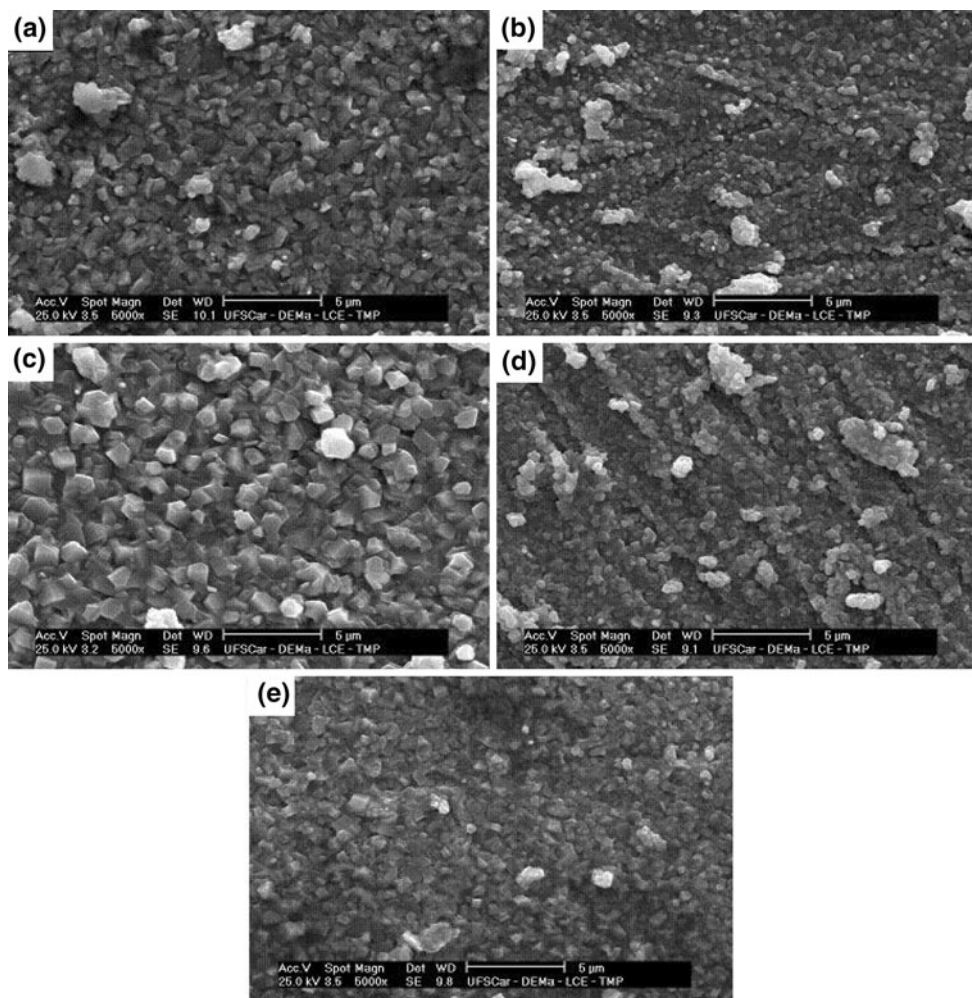
Scanning electron microscopy (SEM) was used to reveal whether a relationship existed between the mannitol concentration and zinc electrodeposit morphology.

Figures 6 and 7 show SEM micrographs of zinc electrodeposits produced chronoamperometrically from −0.60 V to the potential −1.60 V, in the absence or presence of mannitol, with a q_d of 2.0 and 10.0 C cm⁻², respectively.

Figure 6a–e shows that for zinc electrodeposits obtained with q_d 2.0 C cm⁻², the size of the Zn crystallites decreases as the mannitol concentration increases, except at 0.010 M.

Fig. 6 SEM micrographs of Zn films of 2.0 C cm^{-2} obtained chronoamperometrically on a 1010 steel electrode, from -0.60 V to -1.60 V .

Electrolytic solution 0.10 M $\text{ZnSO}_4 + 2.0 \text{ M NaOH}$, with mannitol at concentrations **a** 0.0 M , **b** 0.0050 M , **c** 0.010 M , **d** 0.10 M , and **e** 0.20 M



In this case, hexagonal zinc crystallites can be seen. With the higher q_d of 10.0 C cm^{-2} , the size of Zn crystallites also decreases with increasing mannitol concentration, except at 0.010 M . However, at 10.0 C cm^{-2} , hexagonal zinc crystallites can be seen in all the micrographs, in the presence and absence of mannitol (Fig. 7a–e).

These results suggest that the zinc nucleation mechanism was different in the zinc bath containing 0.010 M mannitol, affecting the deposits at both q_d .

Lee and co-workers [24] investigated the synergistic effects of additives in the improvement of electroplating of zinc at high-current densities (HCD). Thus, they concluded that the synergistic effects on smoothening the deposit surface, refining the grain size, and enhancing the CE of zinc electroplating over a wide range of current densities are attributable to the adsorption of precombined polyoxyethylene nonyl phenyl ether, *o*-chlorobenzyl aldehyde, and polyoxyethylene lauryl amine molecules, and demonstrated a successful Zn-plating solution for the HCD plating process. In another study [25], these researchers investigated zinc deposition from baths containing polyamines: polyethyleneimine (PEI, Lugalvan G35) or the

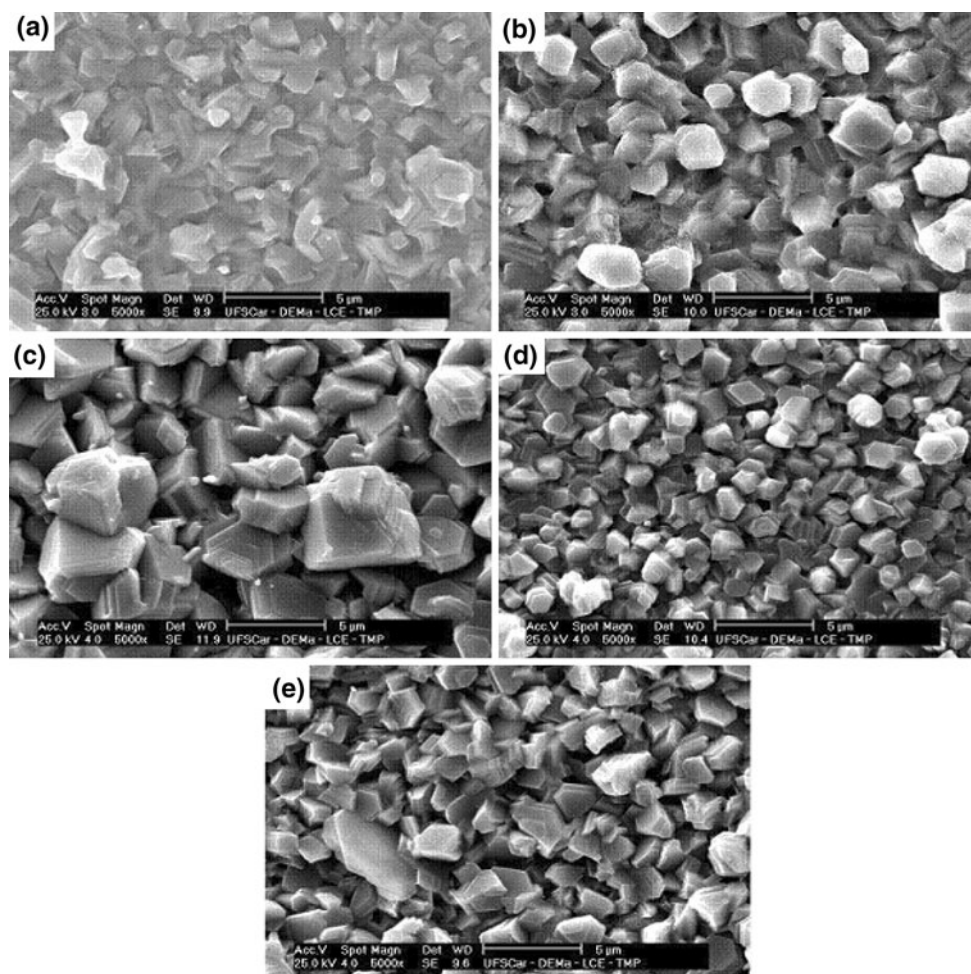
reaction product of imidazole and epihalohydrin (Lugalvan IZE) or polyquaternary amine salt (Lugalvan P), in a HCD process. Also, they showed that the charge density of additives is an important parameter for producing a uniform, smooth, and compact HCD Zn deposit. The adsorption strength of the additives decreased in the order: Lugalvan P > Lugalvan IZE > Lugalvan G35. It was found that a strong synergistic effect of quaternized pyridine carboxylic acid, added to the zinc alkaline bath containing polyamine additives, significantly improved the morphologies of HCD Zn deposits.

The zinc electrodeposits studied here were obtained chronoamperometrically from -0.60 V to -1.60 V , with q_d of 2.0 and 10.0 C cm^{-2} (Figs. 6, 7). It must be stressed that the current density (calculated from the current-time transients) corresponding to this deposition potential, for both q_d , was in the range from ~ 2.1 to 7.8 mA cm^{-2} , which is far lower than those used by Lee and co-workers [24, 25]. Under these deposition conditions, dendrites were not observed.

Finally, it can be concluded that mannitol works as a brightener of zinc electrodeposits, when present in baths at the concentration of 0.10 or 0.20 M , for both q_d .

Fig. 7 SEM micrographs of Zn films of 10.0 C cm^{-2} obtained chronoamperometrically on a 1010 steel electrode, from -0.60 V to -1.60 V .

Electrolytic solution 0.10 M $\text{ZnSO}_4 + 2.0 \text{ M}$ NaOH , with mannitol at concentrations of **a** 0.0 M , **b** 0.0050 M , **c** 0.010 M , **d** 0.10 M , and **e** 0.20 M



3.3 Energy-dispersive X-ray spectroscopy (EDS) analysis of zinc electrodeposits

EDS analysis was performed on the zinc deposits of $q_d 2.0$ and 10.0 C cm^{-2} produced in Zn baths with and without mannitol, at -1.60 V (Table 4).

In Table 4, the presence of oxygen may be noted, due probably to native oxide film and incorporation of O into the zinc deposits during electrodeposition.

Zinc electrodeposits obtained in the presence of mannitol at $\geq 0.10 \text{ M}$ were more refined than at lower mannitol concentrations and also showed oxygen contents that were low or even below the detection limit.

4 Conclusions

The voltammetric deposition and dissolution of zinc on 1010 steel produced in zincate solution without or with mannitol, was characterized by a cathodic wave c_0 and peak c_1 and an anodic peak a_1 of zinc dissolution. Cyclic voltammograms of 1010 steel in zincate solution, in the

Table 4 Zn and O contents of zinc deposited chronoamperometrically at two different q_d from -0.60 V to -1.60 V

Mannitol (M)	EDS (wt%)			
	$q_d 2.0 \text{ C cm}^{-2}$		$q_d 10.0 \text{ C cm}^{-2}$	
	Zn	O	Zn	O
0.0	98.83	1.17 ^a	97.16	2.84
0.0050	95.92	4.07	95.42	4.58
0.010	97.76	2.24	98.48	1.52
0.10	99.01	0.98 ^a	98.62	1.38
0.20	98.55	1.45 ^a	98.70	1.30

Electrolytic solutions 0.10 M $\text{ZnSO}_4 + 2.0 \text{ M}$ NaOH , with various mannitol concentrations

^a Below detection limit

presence and absence of mannitol, with the limit potential at -1.45 V , indicated that the region of wave c_0 corresponds to iron oxide reduction, HER, and first zinc bulk deposition. When the sweep was reversed at -1.60 V , a peak a_1 was seen in the positive sweep, in the absence or presence of mannitol, due to zinc dissolution. This anodic

peak, a_1 , indicates that the primary nucleation and growth of Zn in region c_0 is followed (from ~ -1.52 V) by zinc secondary nucleation and growth. The latter occurs on top of the first zinc layer.

The CE for zinc deposition remained constant (at q_d 2.0 C cm $^{-2}$) or increased (at q_d 10.0 C cm $^{-2}$) with addition of mannitol in the range of concentration from 0 to 0.010 M. However, at both q_d , CE decreased as the mannitol concentration went past 0.10 M. The thickness of the zinc electrodeposits corroborated this pattern of CE values.

SEM results showed that mannitol works as a brightener of zinc electrodeposits, when present in baths at concentrations ≥ 0.10 M, for either deposition charge density. EDS showed the presence of oxygen, which was due probably to native oxide film and incorporation of oxygen into the zinc deposits during electrodeposition.

Acknowledgment The authors gratefully acknowledge CAPES and FAPESP for financial support.

References

- Parthasarathy NV (1989) Practical electroplating handbook. Prentice-Hall, Englewood Cliffs, NJ
- Wranglen G (1960) *Electrochim Acta* 2:130
- Vincent CA, Bonino F, Lazzari M, Scrosati B (1984) Modern batteries: an introduction to electrochemical power sources. Arnold E, London, p 12
- Bockris JO'M, Nagy Z, Drazic D (1973) *J Electrochem Soc* 120:30
- Cachet C, Chami Z, Wiart R (1987) *Electrochim Acta* 32:465
- Blinov VM, Kuprik AV, Gnedenkov VLYU, Loshkarev YUM, Trofimenko VV (1988) *Sov Electrochim* 24:428
- Blinov VM, Burov LM, Trofimenko VV, Gnedenkov LYU, Loshkarev YUM (1989) *Elektrokhimiya* (Sov Electrochim) 25:836
- Sahoo P, Jabakumar KE, Mitragotri DS, Narasimhan SV (1993) *Bull Electrochim* 9:470
- Franklin TC, Williams T, Narayanan TSNS, Guhl R, Hair G (1997) *J Electrochim Soc* 144:3064
- Galvani F, Carlos IA (1997) *Metal Finish* 95:70
- Pereira MS, Barbosa LL, Souza CAC, Moraes ACM, Carlos IA (2006) *J Appl Electrochim* 36:727
- Carlos IA, Matsuo TT, Siqueira JLP, Almeida MRH (2004) *J Power Sources* 132:261
- Broggi RL, Oliveira GM, Barbosa LL, Pallone EMJA, Carlos IA (2006) *J Appl Electrochim* 36:403
- Barbosa LL, Almeida MRH, Carlos RM, Yonashiro M, Oliveira GM, Carlos IA (2005) *Surf Coat Technol* 192:145
- Almeida MRH, Carlos IA, Barbosa LL, Carlos RM, Lima-Neto BS, Pallone EMJA (2002) *J Appl Electrochim* 32:763
- Oliveira EM, Carlos IA (2009) *J Appl Electrochim* 39:1849
- Oliveira EM, Rubin W, Carlos IA (2009) *J Appl Electrochim* 39:1313
- Tulio PC, Carlos IA (2009) *J Appl Electrochim* 39:283
- Flis-Kabulska I, Zakroczymsky T, Flis J (2007) *Electrochim Acta* 52:2966
- Zakroczymsky T, Kleshnya V, Flis J (1998) *J Electrochim Soc* 145:1142
- Fletcher S, Halliday CS, Gates D, Westcott M, Lwin T, Nelson GJ (1983) *Electroanal Chem* 159:267
- Siqueira JLP, Carlos IA (2007) *J Power Sources* 166:519
- Lowenheim FA (1974) Modern electroplating, 2nd edn. Wiley, New York
- Hsieh JC, Hu CC, Lee TC (2008) *J Electrochim Soc* 155:D675
- Hsieh JC, Hu CC, Lee TC (2009) *Surf Coat Technol* 203:3111